Journal of the Optical Society of America A
OPTICS, IMAGE SCIENCE, AND VISION

Tunable birefringence and elliptical polarization eigenmodes in a biplate of two quarter-wave plates

JHON PABÓN, CRISTIAN HERNANDEZ, AND RAFAEL TORRES*

Grupo de Óptica y Tratamiento de Señales, Universidad Industrial de Santander, Bucaramanga, Colombia
**rafael.torres@saber.uis.edu.co*

Received 4 July 2023; revised 6 September 2023; accepted 12 September 2023; posted 14 September 2023; published 26 September 2023

Birefringence of elliptical polarization eigenmodes can be conceptualized as a composite system comprising two distinct media: one with linear polarization eigenmodes and the other with circular polarization eigenmodes. However, the practical realization of such a system often involves the combination of two birefringent quarter-wave plates (QWPs). In this study, our objective is to characterize the variable retardation and variable elliptical polarization eigenmodes exhibited by a biplate consisting of two quarter-wave plates. Additionally, we aim to analyze the geometric properties of the transformation of one state of polarization on the Poincaré sphere, employing the emerging state's curve. This curve corresponds to the intersection between the Poincaré sphere and a cone. The outcomes of our study are presented as a function of the angle between the fast axes of the two QWPs. The findings have the potential to contribute to the configuration of q-plates and facilitate the development of quantum communication protocols.

https://doi.org/10.1364/JOSAA.499731

1. INTRODUCTION

Birefringence is a fundamental property observed in certain materials, wherein each polarization eigenstate experiences distinct refractive indices while propagating through the material. An illustrative example of such materials is quartz, which, depending on the direction of the incident beam relative to the optical axis of the crystal [1], may exhibit birefringence with linear polarization eigenstates (BL) [2,3], circular polarization eigenstates (BC), also called optical activity, and elliptical polarization eigenstates (BE). It is essential to characterize the birefringence and its corresponding eigenmodes in these materials, as it enables a comprehensive understanding of light propagation within them. Moreover, this characterization holds significant value for exploring novel applications that harness these properties.

The utilization of combinations of different birefringent plates has proven to be a highly effective approach for creating elements with adjustable properties [4–6]. A simple yet effective method to generate birefringent plates with elliptical polarization eigenstates is by employing a composite wave plate (CW) [7]. Remarkably, even a combination of two wave plates with linear polarization eigenstates can exhibit optical activity when formed into a CW [8,9]. According to Jones' Theorem I [10,11], a CW can be described as a composition of a birefringent plate with linear polarization eigenstates and another birefringent plate with circular polarization eigenstates [12,13]; other works that yields similar results are [7,14]. These composite wave plates have found practical application in the design of achromatic and superachromatic wave plates [15–19], polarization rotators [20–23], birefringent plates with elliptical polarization eigenstates [7,24,25], and elliptical polarizers [26], among other applications.

Typically, a retarder is characterized by its two polarization eigenstates and its birefringence [27], angular variables that follow the standard sign conventions. However, a recent geometric characterization proposed by Salazar-Torres [28,29] suggests that analyzing the curves of emerging polarization states on the Poincaré sphere can provide valuable insights for experimentally measuring the polarization eigenstates and birefringence of materials. Building on the work by Azzam [30], which focused on BL, a geometric formalism for rotating BE was recently introduced for incident linearly polarized monochromatic beams [31]. Nevertheless, for comprehensive applications, a complete characterization should also consider incident elliptical polarization states. Following a similar approach as with BL in [28], this study investigates the curve of emerging polarization states from a BE, taking into account incident elliptically polarized beams. The ideas are applied in the examination of a CW comprising two QWPs [32–34]. The main objective is to determine the eigenmodes and birefringence as functions of the orientation angles of the QWPs' fast axes. The expressions for the eigenstates and birefringence are derived using the formalism of geometric algebras [14,35,36], which is well suited for the methodology proposed in this study. This geometric algebra formalism

facilitates the vectorial analysis of polarization on the Poincaré sphere, and its advantages have recently been highlighted in the characterization of birefringence in biological tissues [37].

This paper is organized as follows: Section 2 describes the birefringent plates with linear polarization eigenstates. Section 3 presents the geometric algebras. Section 4 describes a biplate composed of two QWPs. Section 5 characterizes the biplate as a birefringent plate with elliptical eigenstates. Section 6 presents a geometric description of the curve of emerging states on the Poincaré sphere for incident elliptical polarized beams. Section 7 presents the experimental results that validate the analytical relations obtained in Section 5. In Section 8, a discussion is developed about the main results, and in Section 9, the final conclusions of this work are exposed.

2. BIREFRINGENT PLATES WITH LINEAR POLARIZATION EIGENSTATES

A BL can be characterized by its curve of emergent states on the Poincaré sphere when a polarized beam is incident. This curve corresponds to the intersection of the Poincaré sphere with a cone, where the angle of the cone (denoted as δ) corresponds to the phase retardation of the birefringent material [28]. In summary we have as follows.

Law of birefringence with linear polarization eigenmodes. *When a polarized light beam passes through a birefringent medium with linear polarization eigenmodes, all the emergent states can be described as belonging to the intersection curve formed by the Poincaré sphere and a cone. The vertex of this cone is in the enantiogyre state of the incident polarization state, the state that has the same azimuth and ellipticity, but the rotation of the electric field is in the opposite direction* (see Fig. 1).

A polarization state $\mathbf{S}(2\alpha, 2\chi)$ with azimuth α and ellipticity χ is represented as a point on the Poincaré sphere, and can be represented by a normalized Stokes vector [38].

Therefore, if a state $\mathbf{S}_{\text{input}}(2\alpha, 2\chi) = (\mathbf{S}_1, \mathbf{S}_2, \mathbf{S}_3)$ passes through a BL, the vertex of the cone is in $(a, b, c) = (\mathbf{S}_1, \mathbf{S}_2, -\mathbf{S}_3)$, and the enantiogyre state $\mathbf{S}_{\text{enant}} = \mathbf{S}(2\alpha, -2\chi)$. Thus, the parametric equations of the cone are

$$\begin{pmatrix} 1 \\ x \\ y \\ z \end{pmatrix} = \begin{pmatrix} 1 \\ a + \left(\frac{1-\cos\delta}{\sin\delta}\right)(z-c)\sin 2t \\ b - \left(\frac{1-\cos\delta}{\sin\delta}\right)(z-c)\cos 2t \\ z \end{pmatrix}, \tag{1}$$

where z and t are independent parameters.

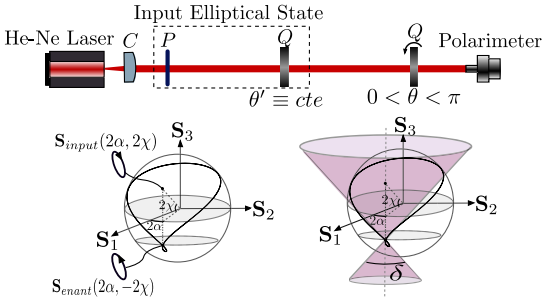

Fig. 1. Optical scheme used by [28] for birefringent plates with linear polarization eigenmodes, where **C** is a collimating lens, **P** is a linear polarizer, $\theta' \equiv cte$ is a constant angle, and **Q**'s are rotating quarter-wave plates.

3. POLARIZATION ON THE BASIS OF PAULI MATRICES

The operators that represent birefringent media are unitary transformations [39], rotations on the Poincaré sphere, where geometric algebras emerge intuitively. On one hand, through the Pauli vectors, proposed by Whitney [40] and extended by Tudor [35,36,41,42], a birefringent medium is expressed as

$$e^{\pm i\hat{n}\cdot\hat{\sigma}\frac{\delta}{2}} = \sigma_0 \cos\frac{\delta}{2} \pm i\hat{n}\cdot\hat{\sigma}\sin\frac{\delta}{2}, \tag{2}$$

where δ is the medium's birefringence, $\sigma_0 = \hat{I}$ is the 2×2 identity matrix, $\hat{n}$ is a Stokes vector associated with the medium's polarization eigenstates, and $\hat{\sigma} = (\sigma_1, \sigma_2, \sigma_3)$ is the Pauli vector. On the other hand, a quaternion formalism was proposed by Richartz and Hsu [43], and extended by Pellat-Finet [14,44], where an operator for birefringent media is presented as $e^{\mathbf{e}_q\frac{\delta}{2}} = \cos\frac{\delta}{2} + \mathbf{e}_q\sin\frac{\delta}{2}$, with linear, elliptical, or circular eigenstates, only varying the rotation axis $\mathbf{e}_q$.

To leverage the geometric characterization of birefringent media, we utilized the formalism of geometric algebras, employing a basis comprising Pauli matrices. This choice of basis enables us to establish an isomorphism with quaternions, thereby unifying both algebraic languages. By adopting geometric algebras, we can more easily analyze the transformations of polarization on the Poincaré sphere, taking advantage of the versatile mathematical framework provided by this approach. Thus, consider the product of quaternions

$$\mathbf{e}_i\mathbf{e}_j = -\delta_{ij} + \varepsilon_{ijk}\mathbf{e}_k, \tag{3}$$

where $\mathbf{e}_i$ $(i = 0, 1, 2, 3)$ is the quaternion basis, and the Pauli vector basis obeys the following product:

$$\sigma_i\sigma_j = \delta_{ij} + i\varepsilon_{ijk}\sigma_k, \tag{4}$$

with $i = \sqrt{-1}$ being the imaginary unit and $\sigma_0 = \hat{I}$ the identity matrix. These two formulations can be unified noticing that

$$(-i\sigma_i)(-i\sigma_j) = -\sigma_i\sigma_j = -\delta_{ij} + \varepsilon_{ijk}(-i\sigma_k), \tag{5}$$

that is, associating $\mathbf{e}_j = -i\sigma_j$ [45,46], one has

$$\underbrace{(-i\sigma_i)}_{\mathbf{e}_i}\underbrace{(-i\sigma_j)}_{\mathbf{e}_j} = -\delta_{ij} + \varepsilon_{ijk}\underbrace{(-i\sigma_k)}_{\mathbf{e}_k}. \tag{6}$$

Therefore, these two representations obey isomorphic algebras, with the base expressed as $\mathbf{e}_j$, being the irreducible representation of the quaternions [47].

A. Birefringent Media in Pauli Vector Formalism

The use of geometric algebra formalism brings about a significant simplification in the treatment of systems comprising multiple wave plates. This simplification arises from the explicit formulation of wave plate operators in terms of their respective eigenstates. To demonstrate this advantage, we will express the operator of a BE, which introduces a retardation γ, described in the form $e^{\mathbf{e}_q\frac{\gamma}{2}} = \cos\frac{\gamma}{2} + \mathbf{e}_q\sin\frac{\gamma}{2}$, where $\mathbf{e}_q$ is defined as

$$\mathbf{e}_q = \mathbf{e}_1\cos 2\chi\cos 2\alpha + \mathbf{e}_2\cos 2\chi\sin 2\alpha + \mathbf{e}_3\sin 2\chi. \tag{7}$$

The special cases with linear and circular polarization eigenstates are determined by the values of α and χ [14,35]. The action of this operator in transforming a polarization state is represented as

$$\hat{\mathbf{S}}' = e^{\mathbf{e}_q \frac{\gamma}{2}} \hat{\mathbf{S}} e^{-\mathbf{e}_q \frac{\gamma}{2}}, \tag{8}$$

where $\hat{\mathbf{S}} = (1, \vec{\mathbf{S}})$ is a state of polarization in the base $\mathbf{e}_i$ (see Appendix A), with $\vec{\mathbf{S}} = \left(\frac{S_1}{S_0}, \frac{S_2}{S_0}, \frac{S_3}{S_0}\right)$ being a pure quaternion, whose elements are the normalized Stokes parameters. More details are shown in Supplement 1.

When $\chi = 0$ in Eq. (7), the case of a BL with eigenstates $\mathbf{e}_l$ and retardation δ is obtained, where the orientation of the fast axis with respect to the horizontal is $\alpha = \theta$, as follows:

$$\mathbf{e}_l = \mathbf{e}_1 \cos 2\theta + \mathbf{e}_2 \sin 2\theta. \tag{9}$$

In this way, $e^{\mathbf{e}_l \frac{\delta}{2}} = \cos\frac{\delta}{2} + \mathbf{e}_l \sin\frac{\delta}{2}$ is obtained.

4. COMPOSITE WAVE PLATES

The composition of several BLs generally produces an equivalent BE [7,24,25]. Thus, by using two QWPs to build a biplate, a birefringent plate can be designed with adjustable elliptical polarization eigenmodes, depending on the angle of separation between the fast axes of the QWPs, as shown in Fig. 2.

Figure 3 shows the experimental scheme for the study of the emergent states generated by the biplate, where θ_m and θ_n are the angles of the fast axes with respect to the horizontal.

Although the biplate can be characterized in the Mueller formalism (see Supplement 1), in this work we want to highlight the geometric relations of these operators on the Poincaré sphere, so we opted for a development in geometric algebras based on Pauli vectors. For the first and second QWPs the indices are m and n, respectively, with linear eigenmodes $\mathbf{e}_m$ and $\mathbf{e}_n$, as Eq. (9), expressed as

$$\mathbf{e}_m = \cos 2\theta_m \mathbf{e}_1 + \sin 2\theta_m \mathbf{e}_2, \tag{10}$$

and

$$\mathbf{e}_n = \cos 2\theta_n \mathbf{e}_1 + \cos 2\theta_n \mathbf{e}_2. \tag{11}$$

The operator of each QWP is written in the form

$$e^{\mathbf{e}_m \frac{\delta_m}{2}} = \frac{\sqrt{2}}{2}(1 + \mathbf{e}_m), \tag{12}$$

and

$$e^{\mathbf{e}_n \frac{\delta_n}{2}} = \frac{\sqrt{2}}{2}(1 + \mathbf{e}_n), \tag{13}$$

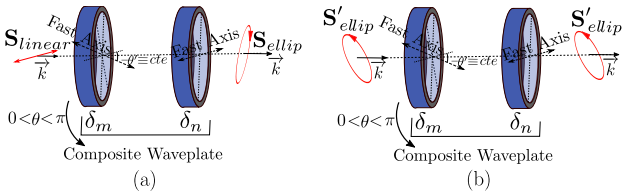

Fig. 2. Biplate composed of two BLs of birefringences δ_n and δ_m, where θ' is the angle between the fast axes. (a) The emergent state is elliptical when the incident state is linear. (b) Elliptical polarization eigenmode of the biplate.

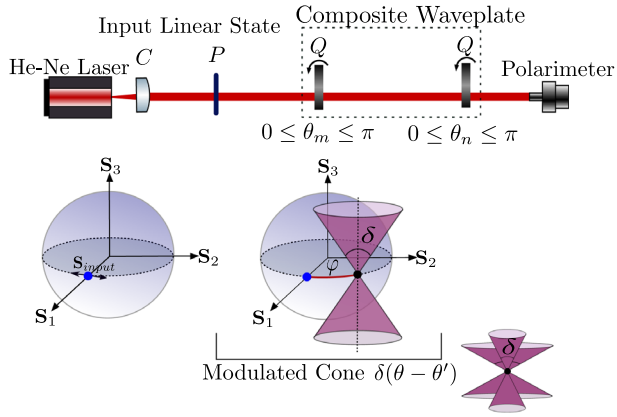

Fig. 3. Optical scheme to capture the curve of emergent polarization states generated by the biplate composed of two QWPs. This curve is generated by the intersection of the Poincaré sphere with a cone of angle δ, where the rotating angle φ is the optical activity of the medium. Here **C** is a collimating lens, **P** is a linear polarizer, and **Q**'s are the QWPs.

where $\delta_m = \delta_n = \frac{\pi}{2}$ is the phase retardation introduced by the first and second QWPs. Defining $\theta' = \theta_n - \theta_m$, the separation between $\mathbf{e}_m$ and $\mathbf{e}_n$ on the Poincaré sphere is given by $2\theta'$. Hence, the dot and vector products between $\mathbf{e}_m$ and $\mathbf{e}_n$ are

$$\mathbf{e}_n \cdot \mathbf{e}_m = \cos 2\theta', \tag{14}$$

and

$$\mathbf{e}_n \times \mathbf{e}_m = -\mathbf{e}_3 \sin 2\theta', \tag{15}$$

and thus, its geometric product is written in the form

$$\mathbf{e}_n \mathbf{e}_m = -\mathbf{e}_n \cdot \mathbf{e}_m + \mathbf{e}_n \times \mathbf{e}_m. \tag{16}$$

The biplate operator composed of two BLs, Eqs. (12) and (13), can be written as a BE operator of the form

$$\mathbf{S}' = \underbrace{e^{\mathbf{e}_n \frac{\pi}{4}} e^{\mathbf{e}_m \frac{\pi}{4}}}_{e^{\mathbf{e}_q \frac{\gamma}{2}}} \mathbf{S} e^{-\mathbf{e}_m \frac{\pi}{4}} e^{-\mathbf{e}_n \frac{\pi}{4}} = e^{\mathbf{e}_q \frac{\gamma}{2}} \mathbf{S} e^{-\mathbf{e}_q \frac{\gamma}{2}}, \tag{17}$$

where γ is the birefringence, of elliptical polarization eigenmodes $\mathbf{e}_q$ of the form Eq. (7). This equation allows obtaining the equalities that analytically characterize the eigenmodes and the birefringence of the biplate. Operating in the previous equation the product of the two QWPs and using Eq. (16), we obtain

$$\begin{aligned} e^{\mathbf{e}_n \frac{\pi}{4}} e^{\mathbf{e}_m \frac{\pi}{4}} &= \frac{1}{2}(1 + \mathbf{e}_n)(1 + \mathbf{e}_m) \\ &= \frac{1}{2}(1 - \mathbf{e}_n \cdot \mathbf{e}_m + \mathbf{e}_m + \mathbf{e}_n + \mathbf{e}_n \times \mathbf{e}_m), \end{aligned} \tag{18}$$

and substituting Eqs. (14) and (15), we obtain

$$e^{\mathbf{e}_n \frac{\pi}{4}} e^{\mathbf{e}_m \frac{\pi}{4}} = \frac{1}{2}(1 - \cos 2\theta' + \mathbf{e}_m + \mathbf{e}_n - \mathbf{e}_3 \sin 2\theta'). \tag{19}$$

Substituting Eqs. (10) and (11) in the above equation (mathematical details are found in Supplement 1), we obtain the biplate operator

$$e^{\mathbf{e}_n \frac{\pi}{4}} e^{\mathbf{e}_m \frac{\pi}{4}} = \sin^2\theta' + \mathbf{e}_1 \cos(2\theta_n - \theta')\cos\theta' + \mathbf{e}_2 \sin(2\theta_n - \theta')\cos\theta' - \mathbf{e}_3 \sin\theta'\cos\theta'. \tag{20}$$

The presence of the term in $\mathbf{e}_3$ indicates that the biplate presents elliptical polarization eigenmodes, which can be expressed in terms of $\mathbf{e}_q$ of the form Eq. (7). Additionally, using Jones' Theorem I [10,11] we can describe the biplate as the composition of a BL and an optical activity or BC.

Based on the above, we will characterize the biplate operator of two QWPs, on one hand as a BE and on the other hand by means of Jones' Theorem I, in the geometric algebra formalism [14]. This double characterization is written in the form

$$e^{\mathbf{e}_n \frac{\pi}{4}} e^{\mathbf{e}_m \frac{\pi}{4}} = e^{\mathbf{e}_l \frac{\delta}{2}} e^{\mathbf{e}_3 \frac{\varphi}{2}} = e^{\mathbf{e}_q \frac{\gamma}{2}}, \tag{21}$$

and substituting the biplate operator expressed in Eq. (20), we obtain Eq. (22), which provides by double equality all the relations between the biplate operator and the six analytical parameters that characterize it as a BE, and as a BL with BC compounds. Details of the mathematical procedure are presented in Supplement 1:

$$\underbrace{\begin{pmatrix} \sin^2\theta' \\ \mathbf{e}_1\left[\cos\left(2\theta_n - \theta'\right)\cos\theta'\right] \\ \mathbf{e}_2\left[\sin\left(2\theta_n - \theta'\right)\cos\theta'\right] \\ \mathbf{e}_3\left[-\sin\theta'\cos\theta'\right] \end{pmatrix}}_{e^{\mathbf{e}_n \frac{\pi}{4}} e^{\mathbf{e}_m \frac{\pi}{4}}} = \underbrace{\begin{pmatrix} \cos\frac{\delta}{2}\cos\frac{\varphi}{2} \\ \mathbf{e}_1\left[\sin\frac{\delta}{2}\cos\left(2\alpha' - \frac{\varphi}{2}\right)\right] \\ \mathbf{e}_2\left[\sin\frac{\delta}{2}\sin\left(2\alpha' - \frac{\varphi}{2}\right)\right] \\ \mathbf{e}_3\left[\cos\frac{\delta}{2}\sin\frac{\varphi}{2}\right] \end{pmatrix}}_{e^{\mathbf{e}_l \frac{\delta}{2}} e^{\mathbf{e}_3 \frac{\varphi}{2}}}$$

$$= \underbrace{\begin{pmatrix} \cos\frac{\gamma}{2} \\ \mathbf{e}_1\left[\cos 2\chi\cos 2\alpha\sin\frac{\gamma}{2}\right] \\ \mathbf{e}_2\left[\cos 2\chi\sin 2\alpha\sin\frac{\gamma}{2}\right] \\ \mathbf{e}_3\left[\sin 2\chi\sin\frac{\gamma}{2}\right] \end{pmatrix}}_{e^{\mathbf{e}_q \frac{\gamma}{2}}}. \tag{22}$$

5. BIPLATE AS A BE

In this section, we proceed to obtain the three parameters that describe a biplate composed of two QWPs as a BE, by solving an equality from Eq. (22), expressed as follows:

$$e^{\mathbf{e}_n \frac{\pi}{4}} e^{\mathbf{e}_m \frac{\pi}{4}} = e^{\mathbf{e}_q \frac{\gamma}{2}}, \tag{23}$$

where γ is the retardation introduced between the elliptical polarization eigenstates $\mathbf{e}_q$. In Supplement 1, the expressions of the biplate as a BE are obtained using the variables (χ, α, γ). The obtained expression for the retardation γ is

$$\cos\frac{\gamma}{2} = \sin^2\theta'. \tag{24}$$

The eigenstates are defined by $\mathbf{e}_q$ expressed in Eq. (7). The values for the azimuthal angle 2α and the ellipticity 2χ are

$$2\alpha = 2\theta_n - \theta', \tag{25}$$

and

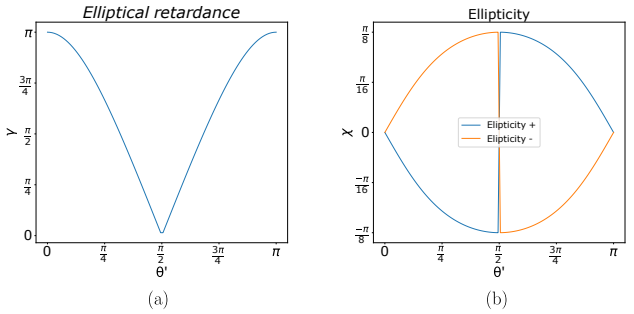

Fig. 4. (a) BE values of γ and (b) ellipticity of its eigenmodes χ, which are variables for the biplate as a function of the difference angle between the fast axes θ'.

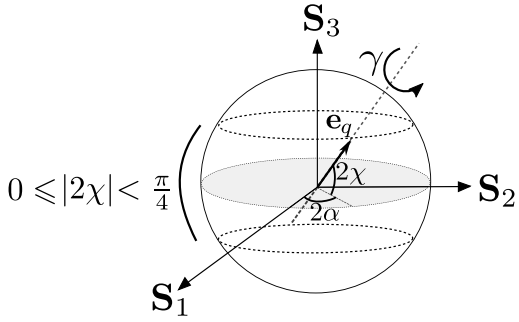

Fig. 5. Wave plate pair acts as a birefringent medium with elliptical polarization eigenstates, characterized by (χ, α). The ellipticity values for the eigenstates of the biplate are limited.

$$\sin 2\chi = \frac{-\sin\theta'\cos\theta'}{\sin(\arccos(\sin^2\theta'))}. \tag{26}$$

Equations (24) and (26) are plotted in Fig. 4. The ellipticity of the biplate's polarization eigenstates varies in the range of $0 \le |\chi| < \frac{\pi}{8}$, as shown in Fig. 5. Thus, not all ellipticity values can be obtained; therefore, a CW composed of two QWPs cannot have circular eigenstates.

A. Biplate as a Composition of Birefringent Plates with Linear and Circular Eigenstates

Now, we proceed to obtain the three parameters that describe a biplate composed of two QWPs using Jones' Theorem I [10,11] as a composition of a BL and optical activity or a BC. We solve the other part of the equality in Eq. (22), expressed in the form

$$e^{\mathbf{e}_n \frac{\pi}{4}} e^{\mathbf{e}_m \frac{\pi}{4}} = e^{\mathbf{e}_l \frac{\delta}{2}} e^{\mathbf{e}_3 \frac{\varphi}{2}}, \tag{27}$$

where φ is the retardation introduced by the optical activity or BC and δ the retardation associated with the BL with eigenstates given by $\mathbf{e}_l = \mathbf{e}_1 \cos 2\alpha' + \mathbf{e}_2 \sin 2\alpha'$. This composition is graphically represented in Fig. 6.

Through the relations expressed in Supplement 1, the expressions for $(\delta, \varphi, \alpha')$ that describe the biplate using Jones' Theorem I as expressed in Eq. (27) are determined. The mathematical details can be found in Supplement 1. For the BL, the retardation obtained is

$$\delta = \pi - 2\theta', \tag{28}$$

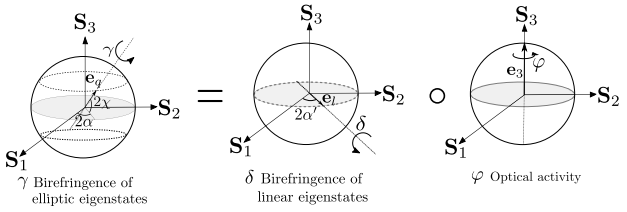

Fig. 6. Birefringent medium with elliptical eigenstates characterized by (γ, χ, α), described by the composition of a birefringent medium of linear polarization eigenstates with retardation δ and orientation of $2\alpha'$, and an optical activity whose retardation is φ.

with eigenstates given by

$$\mathbf{e}_l = \mathbf{e}_1 \cos 2\alpha' + \mathbf{e}_2 \sin 2\alpha', \tag{29}$$

and the orientation angle is

$$2\alpha' = 2\theta_n - \frac{\pi}{2}. \tag{30}$$

For the optical activity or BC, we get the following retardation:

$$\varphi = 2\theta' - \pi. \tag{31}$$

It is important to point out the constraints that exist between the different angles that characterize the biplate:

$$\delta = -\varphi, \tag{32}$$

and

$$\frac{\delta}{2} + \theta' = \frac{\pi}{2}. \tag{33}$$

Therefore, the angle between the fast axes θ' of the two QWPs completely determines the resulting BE. In this way, the expressions of the six parameters that describe the biplate as a BE were determined.

6. GEOMETRIC CHARACTERIZATION OF BE ON THE POINCARÉ SPHERE

Birefringent media exhibit distinct transformations that depend on their retardation and eigenmodes. In a previous study, Salazar-Torres [28] characterized the curve of emergent states for BL by a cone that intersects the Poincaré sphere. Extending this geometric approach suggests that the BEs also have a geometric characterization of their emergent states on the Poincaré sphere. So, the emergent states of a BE with incident polarized light are written in the form

$$\hat{\mathbf{S}}' = e^{\mathbf{e}_q \frac{\gamma}{2}} \hat{\mathbf{S}} e^{-\mathbf{e}_q \frac{\gamma}{2}}, \tag{34}$$

where α and χ are the azimuth and polarization ellipticity of the incident beam $\hat{\mathbf{S}}$, respectively.

By Jones' Theorem I [10,11], the operator of a BE of eigenmodes $\mathbf{e}_q$ is decomposed as the composition of two birefringent plates, a BL of eigenstates $\mathbf{e}_l$, and an optical activity or BC of $\mathbf{e}_3$ eigenstates, expressed in the form [14]

$$e^{\mathbf{e}_q \frac{\gamma}{2}} = e^{\mathbf{e}_l \frac{\delta}{2}} e^{\mathbf{e}_3 \frac{\varphi}{2}}, \tag{35}$$

and therefore

$$e^{-\mathbf{e}_q \frac{\gamma}{2}} = e^{-\mathbf{e}_3 \frac{\varphi}{2}} e^{-\mathbf{e}_l \frac{\delta}{2}}, \tag{36}$$

where $e^{-\mathbf{e}_q \frac{\gamma}{2}} = e^{(\mathbf{e}_q \frac{\gamma}{2})^\dagger}$, and $\dagger$ is the conjugate adjoint, which allows describing Eq. (34) in the form

$$\hat{\mathbf{S}}' = e^{\mathbf{e}_l \frac{\delta}{2}} \underbrace{e^{\mathbf{e}_3 \frac{\varphi}{2}} \hat{\mathbf{S}}(2\alpha, 2\chi) e^{-\mathbf{e}_3 \frac{\varphi}{2}}}_{\mathbf{S}(2\alpha+\varphi, 2\chi)} e^{-\mathbf{e}_l \frac{\delta}{2}}. \tag{37}$$

Operating the BC in the incident state (see Appendix B), the following was obtained:

$$\hat{\mathbf{S}}' = e^{\mathbf{e}_l \frac{\delta}{2}} \hat{\mathbf{S}}(2\alpha + \varphi, 2\chi) e^{-\mathbf{e}_l \frac{\delta}{2}}, \tag{38}$$

which corresponds to the action of a BL on a state with $2\alpha' = 2\alpha + \varphi$. Equation (38) is solved in Appendix C, where the emergent states are obtained in the form

$$\begin{aligned}
&\mathbf{e}_0 \mathbf{S}'_0 + \mathbf{e}_1 \mathbf{S}'_1 + \mathbf{e}_2 \mathbf{S}'_2 + \mathbf{e}_3 \mathbf{S}'_3 \\
&= \mathbf{e}_0 + \mathbf{e}_1 (\cos 2\chi \cos 2\alpha' + [\cos 2\chi \sin(2\alpha' - 2\theta)(1 - \cos\delta) \\
&\quad \pm \sin 2\chi \sin\delta] \sin 2\theta) + \mathbf{e}_2 (\cos 2\chi \sin 2\alpha' \\
&\quad - [\cos 2\chi \sin(2\alpha' - 2\theta)(1 - \cos\delta) \pm \sin 2\chi \sin\delta] \cos 2\theta) \\
&\quad + \mathbf{e}_3 (\pm \sin\delta \cos 2\chi \sin(2\alpha' - 2\theta) + \sin 2\chi \cos\delta).
\end{aligned} \tag{39}$$

The above equation was previously characterized as the parametric equations of a cone that intersects the Poincaré sphere [28]. Therefore, the equation of emergent states generated by a BE presents the same mathematical structure; its emergent states are also determined by a cone of angle δ, but with its vertex rotated due to the rotating power caused by optical activity or BC φ. The cone, therefore, has the form of Eq. (1), with the variant that the vertex of the cone is $(a, b, c) = \mathbf{S}(2\alpha + \varphi, -2\chi)$, and then

$$\begin{pmatrix} 1 \\ x \\ y \\ z \end{pmatrix} = \begin{pmatrix} 1 \\ \cos 2\chi \cos(2\alpha + \varphi) + \left(\frac{1-\cos\delta}{\sin\delta}\right)(z + \sin 2\chi) \sin 2t \\ \cos 2\chi \sin(2\alpha + \varphi) - \left(\frac{1-\cos\delta}{\sin\delta}\right)(z + \sin 2\chi) \cos 2t \\ z \end{pmatrix}. \tag{40}$$

So it turns out that its input state $\mathbf{S}_{\text{input}}(2\alpha, 2\chi)$ also determines the vertex of the cone for a BE, $\mathbf{S}_{\text{crosses}}(2\alpha', -2\chi)$. The state that determines the vertex of the cone is expressed in the form

$$\mathbf{S}_{\text{cross}}(2\alpha', -2\chi) = \mathbf{S}(2\alpha + \varphi, -2\chi). \tag{41}$$

This results in the geometric law of birefringence with elliptical polarization eigenmodes.

Law of birefringence with elliptical polarization eigenmodes. *The emergent states resulting from the propagation of a polarized light beam through a birefringent medium, characterized by elliptical polarization eigenmodes, belong to the intersection curve formed by the Poincaré sphere and a rotated cone. The rotation of this cone is determined by the optical activity, while the cone itself represents the birefringence associated with linear polarization eigenmodes.*

No queda claro respecto de qué eje se rota el cono

Said law is represented in Fig. 7; when the optical activity is null $\varphi = 0$, all the expressions converge to the law of the BL [28],

Luego se tendrá que hablar sobre la rotación del cono respecto al eje S1

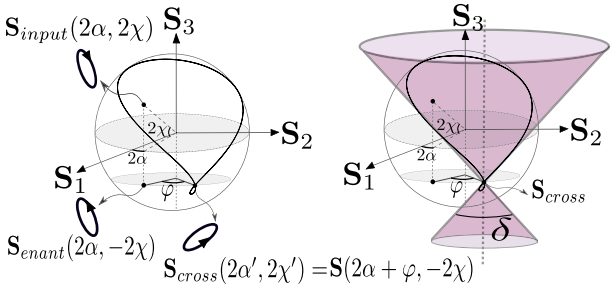

Fig. 7. Representation of the law of BE, and the relation between the input state $\mathbf{S}_{\text{input}}$ with the cross $\mathbf{S}_{\text{cross}}$, which determines the vertex of the cone.

and if the linear birefringence is null $\delta = 0$, the model reduces to the case of a BC.

A. Cases of Special Practical Interest

Using Expressions Eq. (28)–(31), the corresponding CW can be calculated for some particular cases.

1. CW with $\theta' = 0$

In this case, it results in a birefringent plate with rotational power given by $\varphi = -\pi$. Therefore, its effect is equivalent to a BL with birefringence $\delta = \pi$. Thus, its eigenmodes are $\mathbf{e}_l = \mathbf{e}_1 \sin 2\theta_n - \mathbf{e}_2 \cos 2\theta_n$.

2. CW with $\theta' = \pi/2$

In this case, the biplate converges to the identity operator in Eq. (20). It results in a birefringent plate with rotational power $\varphi = 0$. Therefore, its effect is equivalent to a BL with birefringence $\delta = 0$, where its eigenmodes are $\mathbf{e}_l = -\mathbf{e}_1 \sin 2\theta_n + \mathbf{e}_2 \cos 2\theta_n$.

3. CW with $\theta' = \pi/4$

In this case, it results in a birefringent plate with rotational power given by $\varphi = -\pi/2$, plus the effect of a BL with birefringence $\delta = \pi/2$ and eigenmodes $\mathbf{e}_l = \mathbf{e}_1 \cos 2\theta_n + \mathbf{e}_2 \sin 2\theta_n$.

7. EXPERIMENTS AND RESULTS

With the purpose of verifying the expressions previously obtained for the biplate, an experimental setup was proposed, illustrated in Fig. 3, to capture the emerging states. For this, we use a He–Ne laser ($\lambda = 632.8$ [nm]), filtered and collimated, along with two commercial QWPs from Thorlabs as shown in Fig. 2. Both QWPs were mounted on a mechanical device that allows them to be rotated synchronously while maintaining the angle θ' between the fast axes of the QWPs. The beam passes through a linear polarizer $\mathbf{P}$ and the respective wave plate. The QWPs are rotated from 0° to 180°, in steps of 2°, registering 90 emerging states. These were measured with the commercial Thorlabs polarimeter (PAN5710VIS, S/N: M00255491). Three incident states were used, a linearly and two elliptically polarized states, recorded in Table 1, where $\bar{\alpha}$ and $\bar{\chi}$ represent the experimental average of the azimuthal and elliptical angles, respectively, of the Stokes vector $\mathbf{S}(2\alpha, 2\chi) = (\mathbf{S}_1, \mathbf{S}_2, \mathbf{S}_3)$. For each emerging state, 100 data were measured.

Table 1. Values of Azimuth α and Ellipticity χ of the States Incident on the Biplate

	$\bar{\chi}° \pm 0.25°$	$\bar{\alpha}° \pm 0.25°$
$\mathbf{S}_H$	0.01	−0.33
$\mathbf{S}_{\text{ellip1}}$	20.18	−45.07
$\mathbf{S}_{\text{ellip2}}$	20.28	45.06

By varying θ', five different variants were generated with values of $\theta' = 0°, 30°, 54°, 80°, 90°$. These were illuminated with a linearly polarized state, and their curves of emerging states was recorded. Finally, one of the previously characterized variants with $\theta' = 54°$ was illuminated, and two elliptical states were incident such that they were its eigenstates.

A. Input Linear Polarized State with $\theta' = 0, \pi/2$

First, a horizontal polarized state $\mathbf{S}_{\text{in}} = \mathbf{S}_H$, recorded in Table 1, was incident on the biplate. In the configurations corresponding to the extreme cases of $\theta' = 0° \pm 2°$ and $\theta' = 90° \pm 2°$, their curves of emerging states obtained experimentally were recorded. Theoretically, these curves described by $\mathbf{S}'(\theta_n, \theta')$ are determined by Eq. (17) through Eq. (20). In Fig. 8, these curves of the theoretical emerging states are plotted in blue, experimental ones in red, and the incident state $\mathbf{S}_H$ in black.

The curve on the left in Fig. 8, corresponding to the $\theta' = 0°$ configuration expressed in case A.1, Section 6, is similar to the curve generated by a rotating HWP. It presents a BL with a value equal to a HWP and maintains its linear polarization eigenstates; however, there is an additional optical activity. On the other hand, the right in Fig. 8 corresponds to the $\theta' = 90°$ configuration in case A.2, Section 6. In the latter, there are no changes in the incident polarization state. Since the retardation is null, the biplate operator of Eq. (20) converges to the identity operator.

B. Input Linear Polarized State with $0 < \theta' < \pi/2$

Since δ and θ' have a geometrical interpretation as they make up complementary angles [see Eq. (33)], to experimentally validate this variation of the BL, we generated three curves of emerging states for three biplates with values of $\theta' = 30° \pm 2°$, $\theta' = 54° \pm 2°$, and $\theta' = 80° \pm 2°$. Applying Eq. (28), we obtain

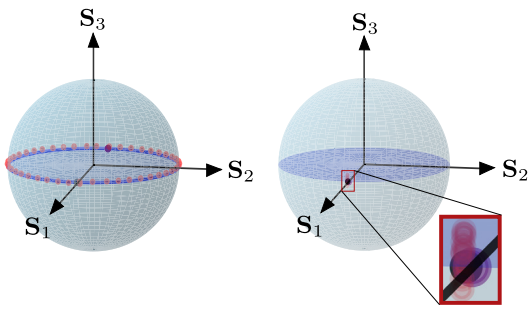

Fig. 8. Curve of emerging states generated by a composite biplate for angles $\theta' = 0° \pm 2°$ and $\theta' = 90° \pm 2°$ in the left and right images, respectively.

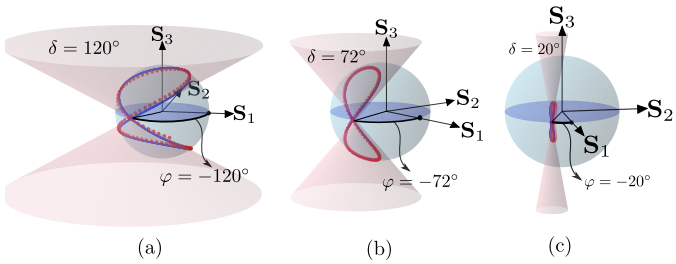

Fig. 9. BL of value δ and optical activity BC of value φ for three biplates with angles (a) $\theta' = 30°$, (b) $\theta' = 54°$, and (c) $\theta' = 80°$.

BLs of $\delta = 120° \pm 2°$, $\delta = 72° \pm 2°$, and $\delta = 20° \pm 2°$, respectively.

Likewise, for the same case studies, the optical activity or BC is evaluated, which is related to the BL in the biplate according to Eq. (32). Thus, BCs of $\varphi = -120° \pm 2°$, $\varphi = -72° \pm 2°$, and $\varphi = -20° \pm 2°$ are obtained, respectively, for these configurations of the biplate. As shown in Fig. 9, the greater the retardation δ, the greater the rotary power φ of the biplate.

C. Input Elliptical Polarized States

On one hand, two elliptical polarization states were experimentally found to be the eigenstates of the biplate for $\theta' = 54°$. The found states were labeled as $\mathbf{S}_{\text{ellip}j}$ for $j = 1, 2$ and are registered in Table 1. On the other hand, the theoretical characterization of the elliptical polarization eigenstates of the biplate was tested through Eqs. (25) and (26), corresponding to their azimuth and ellipticity values, respectively. These are determined by the angles θ' and θ_n. Their theoretical values are registered in Table 2 with their respective percentage error when compared with the experimentally obtained elliptical polarization eigenstates in Table 1. The origin of the error is associated with the uncertainty in polarization states, the precision of the polarimeter, and the quality of the quarter-wave plates.

In Figs. 10 and 11, the theoretical and experimental curves of the emergent states for each incident elliptical polarization state are plotted, along with the polarization ellipses of the incident states and the emergent states corresponding to their eigenstates. These were plotted using the Python Polarization Py_pol package [48], which requires the azimuthal and elliptical angles of the states as input, reported in Table 1 for the incident state. The output eigenstates were extracted from the curve of emergent states obtained experimentally.

In the same graphs, the law of BE is tested. For this, a cone with opening δ expressed in Eq. (28) corresponding to the BL is plotted. The vertex of the cone is defined by the state $\mathbf{S}_{\text{cross}}$ from Eq. (41), which depends on the angular values of the azimuth and ellipticity of the incident state and the BC determined in Eq. (31). Therefore, we obtain

Table 2. Predicted Azimuth α and Ellipticity χ Values for the Eigenstates of the Biplate with $\theta' = 54°$

$\mathbf{S}_{\text{eigenstate}}$	θ_n	$\alpha(\theta_n, \theta')$	$\epsilon\% \pm \delta\epsilon$	$\chi(\theta')$	$\epsilon\% \pm \delta\epsilon$
$\mathbf{S}_{\text{ellip1}}$	-72	-45	$0.4\% < \bar{\epsilon}\% < 0.7\%$	19.48	$2.3\% < \bar{\epsilon}\% < 4.8\%$
$\mathbf{S}_{\text{ellip2}}$	18	45	$0.4\% < \bar{\epsilon}\% < 0.6\%$	19.48	$2.8\% < \bar{\epsilon}\% < 5.3\%$

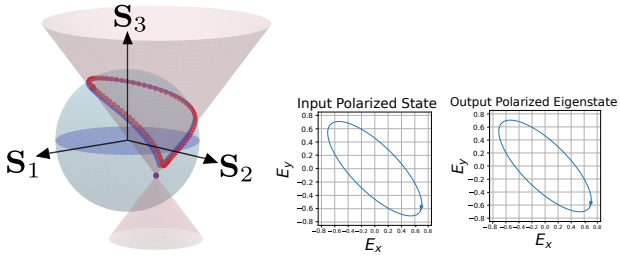

Fig. 10. (a) Theoretical and experimental state curve for the biplate with $\theta' = 54°$ when the elliptical state $\mathbf{S}_{\text{ellip1}}$ is incident upon it. (b), (c) Polarization ellipses of the incident state $\mathbf{S}_{\text{ellip1}}$ and its corresponding emergent eigenstate, respectively.

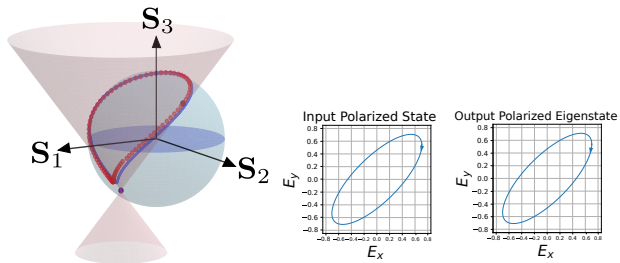

Fig. 11. (a) Theoretical and experimental state curve for the biplate with $\theta' = 54°$ when the elliptical state $\mathbf{S}_{\text{ellip2}}$ is incident upon it. (b), (c) Polarization ellipses of the incident state $\mathbf{S}_{\text{ellip2}}$ and its corresponding emergent eigenstate, respectively.

$$\mathbf{S}_{\text{cross}}(2\alpha', 2\chi') = \mathbf{S}(2\alpha + 2\theta' - \pi, -2\chi), \tag{42}$$

which determines the position of the cone on the Poincaré sphere for the biplate.

8. DISCUSSION

The birefringence and polarization eigenmodes of a biplate were examined, demonstrating that they are adjustable functions dependent on the angle θ' between the fast axes of two QWPs. However, it should be noted that not all ellipticity values of the eigenmodes were observed due to the biplate's inability to achieve configurations with eigenstates having ellipticities greater than $|\chi| > \frac{\pi}{8}$. It is crucial to emphasize that the permissible range of ellipticity values for the eigenmodes is $[0, \frac{\pi}{8})$ for θ' in the range $[0, \pi]$, where the value of $\chi = \frac{\pi}{8}$ is outside of range. When $\theta' \to \pi$, the ellipticity $\chi \to \frac{\pi}{8}$. However, for

$\chi(\theta'=\pi)$ in Eq. (26), the eigenmodes are not defined as shown in Fig. 4(b). This is because in $\theta'=\pi$, the biplate operator converges to the identity. This implies that the birefringence parameters cannot be modified independently, and careful consideration of the angle θ' is necessary to achieve the desired eigenmodes.

Here we want to highlight that current advances underscore the importance of employing geometric algebras, specifically emphasizing the Pellat-Finet quaternion polarization formulation [14,44]. This approach deserves special attention, as it gave us the ability to intuitively anticipate several of the discoveries within our research, further reinforcing the importance of their choice.

9. CONCLUSIONS

A comprehensive characterization of a biplate comprising quarter-wave plates has been successfully accomplished, establishing it as a birefringent medium with elliptical polarization eigenmodes. This formulation, notable for its simplicity, enhances its appeal in both academic research and practical applications. Expression Eq. (22) enabled us to derive the birefringence and eigenstates as a function of the angle between the fast axes of the QWPs. This mechanism provides a means to adjust and tune the properties of the biplate. Furthermore, a geometric law concerning the Poincaré sphere has been discovered for birefringent media with elliptical polarization eigenmodes. According to this law, the emergent state of a polarized beam corresponds to the intersection curve formed by a cone and the Poincaré sphere. Notably, the rotary power manifests as a rotation of the cone's vertex from the enantiogyre polarization state of the incident beam.

APPENDIX A: POLARIZED STATES

The polarized states are represented by the Stokes parameters of the form $\hat{\mathbf{S}}=(\mathbf{S}_0,\mathbf{S}_1,\mathbf{S}_2,\mathbf{S}_3)$, which, when normalized with respect to $\mathbf{S}_0$, obtains a vector of the form $\hat{\mathbf{S}}=(1,\vec{\mathbf{S}})$, where the vector part $\vec{\mathbf{S}}=(\frac{\mathbf{S}_1}{\mathbf{S}_0},\frac{\mathbf{S}_2}{\mathbf{S}_0},\frac{\mathbf{S}_3}{\mathbf{S}_0})$ is a Stokes vector. In the opted Pauli vector notation, it is represented as

$$\hat{\mathbf{S}}=\mathbf{S}_0+\mathbf{e}_1\mathbf{S}_1+\mathbf{e}_2\mathbf{S}_2+\mathbf{e}_3\mathbf{S}_3, \tag{A1}$$

where the scalar part $\mathbf{S}_0$ represents the intensity of the source, and the parts $\mathbf{S}_i$ for $i=1,2,3$ characterize the vector part of the polarization state.

APPENDIX B: BC OR OPTICAL ACTIVITY

By applying the operator corresponding to the optical activity to a polarized state $\hat{\mathbf{S}}(2\alpha,2\chi)$, we obtain

$$\begin{aligned}e^{\mathbf{e}_3\frac{\varphi}{2}}\hat{\mathbf{S}}(2\alpha,2\chi)e^{-\mathbf{e}_3\frac{\varphi}{2}}&=\left(\cos\frac{\varphi}{2}+\mathbf{e}_3\sin\frac{\varphi}{2}\right)\\&\times(1+\mathbf{e}_1\mathbf{S}_1+\mathbf{e}_2\mathbf{S}_2+\mathbf{e}_3\mathbf{S}_3)\\&\times\left(\cos\frac{\varphi}{2}-\mathbf{e}_3\sin\frac{\varphi}{2}\right),\end{aligned} \tag{B1}$$

and solving the multiplication of the three quaternions, we obtain:

$$\begin{aligned}&\cos^2\frac{\varphi}{2}-\sin\frac{\varphi}{2}\cos\frac{\varphi}{2}\sin2\chi+\sin\frac{\varphi}{2}\cos\frac{\varphi}{2}\sin2\chi+\sin^2\frac{\varphi}{2}\\&+\mathbf{e}_1\left[\cos2\chi\left(\cos2\alpha\left(\cos^2\frac{\varphi}{2}-\sin^2\frac{\varphi}{2}\right)-2\sin\frac{\varphi}{2}\cos\frac{\varphi}{2}\sin2\alpha\right)\right]\\&+\mathbf{e}_2\left[\cos2\chi\left(\sin2\alpha\left(\cos^2\frac{\varphi}{2}-\sin^2\frac{\varphi}{2}\right)+2\sin\frac{\varphi}{2}\cos\frac{\varphi}{2}\cos2\alpha\right)\right]\\&+\mathbf{e}_3\left[-\cos\frac{\varphi}{2}\sin\frac{\varphi}{2}+\sin^2\frac{\varphi}{2}\sin2\chi+\cos^2\frac{\varphi}{2}\sin2\chi+\sin\frac{\varphi}{2}\cos\frac{\varphi}{2}\right].\end{aligned} \tag{B2}$$

Applying the identities $\cos\varphi=(\cos^2\frac{\varphi}{2}-\sin^2\frac{\varphi}{2})$ and $\sin\varphi=2\sin\frac{\varphi}{2}\cos\frac{\varphi}{2}$ and the properties of $\sin(A+B)$ and $\cos(A+B)$, we obtain

$$\begin{aligned}e^{\mathbf{e}_3\frac{\varphi}{2}}\mathbf{S}(2\alpha,2\chi)e^{-\mathbf{e}_3\frac{\varphi}{2}}&=1+\mathbf{e}_1\cos2\chi\cos(2\alpha+\varphi)\\&+\mathbf{e}_2\cos2\chi\sin(2\alpha+\varphi)+\mathbf{e}_3\sin2\chi\\&=\mathbf{S}(2\alpha+\varphi,2\chi).\end{aligned} \tag{B3}$$

The above equation represents that an incident polarized state in a medium with optical activity transforms the azimuthal of the incident state with a rotating power maintaining its ellipticity.

APPENDIX C: MATHEMATICAL DEVELOPMENT OF THE LAW OF BE

The transformation of an incident polarized state $\mathbf{S}(2\alpha,2\chi)$ into a BE in Pauli vector formalism is described as

$$\hat{\mathbf{S}}'=e^{\mathbf{e}_l\frac{\delta}{2}}e^{\mathbf{e}_3\frac{\varphi}{2}}\hat{\mathbf{S}}(2\alpha,2\chi)e^{-\mathbf{e}_3\frac{\varphi}{2}}e^{-\mathbf{e}_l\frac{\delta}{2}}, \tag{C1}$$

and operating the optical activity expressed in Eq. (B3), we get

$$\hat{\mathbf{S}}'=e^{\mathbf{e}_l\frac{\delta}{2}}\hat{\mathbf{S}}(2\alpha',2\chi)e^{-\mathbf{e}_l\frac{\delta}{2}}, \tag{C2}$$

where $2\alpha'=2\alpha+\varphi$. Therefore, it is identified that the operator of a BE described by Jones' Theorem I is reduced to the action of operating a BL to the rotated incident state. Therefore, it is obtained that the emergent states are equivalent to those generated by a BL when an incident state $\hat{\mathbf{S}}(2\alpha',2\chi)$ passes through it. Expressing Eq. (C2) of the form

$$\begin{aligned}&\mathbf{S}'_0+\mathbf{e}_1\mathbf{S}'_1+\mathbf{e}_2\mathbf{S}'_2+\mathbf{e}_3\mathbf{S}'_3\\&=\left(\cos\frac{\delta}{2}+\mathbf{e}_1\cos2\theta\sin\frac{\delta}{2}+\mathbf{e}_2\sin2\theta\sin\frac{\delta}{2}\right)\\&\times(1+\mathbf{e}_1\mathbf{S}_1+\mathbf{e}_2\mathbf{S}_2+\mathbf{e}_3\mathbf{S}_3)\\&\times\left(\cos\frac{\delta}{2}-\mathbf{e}_1\cos2\theta\sin\frac{\delta}{2}-\mathbf{e}_2\sin2\theta\sin\frac{\delta}{2}\right),\end{aligned} \tag{C3}$$

operating the three quaternions, and factoring the Stokes parameters, we obtain

$$\mathbf{S}'_0=1, \tag{C4}$$

$$\begin{aligned}\mathbf{S}'_1=\mathbf{S}_1&\left(\cos^22\theta\sin^2\frac{\delta}{2}+\cos^2\frac{\delta}{2}-\sin^22\theta\sin^2\frac{\delta}{2}\right)\\&+2\mathbf{S}_2\cos2\theta\sin2\theta\sin^2\frac{\delta}{2}+2\mathbf{S}_3\sin2\theta\sin\frac{\delta}{2}\cos\frac{\delta}{2},\end{aligned} \tag{C5}$$

$$\mathbf{S}_2' = 2\mathbf{S}_1 \cos 2\theta \sin 2\theta \sin^2\frac{\delta}{2} - 2\mathbf{S}_3 \cos 2\theta \sin\frac{\delta}{2}\cos\frac{\delta}{2} + \mathbf{S}_2\left(\sin^2 2\theta \sin^2\frac{\delta}{2} + \cos^2\frac{\delta}{2} - \cos^2 2\theta \sin^2\frac{\delta}{2}\right), \tag{C6}$$

$$\mathbf{S}_3' = -2\mathbf{S}_1 \sin 2\theta \sin\frac{\delta}{2}\cos\frac{\delta}{2} + 2\mathbf{S}_2 \cos 2\theta \sin\frac{\delta}{2}\cos\frac{\delta}{2} + \mathbf{S}_3\left(-\sin^2 2\theta \sin^2\frac{\delta}{2} + \cos^2\frac{\delta}{2} - \cos^2 2\theta \sin^2\frac{\delta}{2}\right). \tag{C7}$$

Substituting the Stokes parameters and applying the trigonometric relations $\sin^2\frac{\delta}{2} = \frac{1-\cos\delta}{2}$ y $\cos^2\frac{\delta}{2} = \frac{1+\cos\delta}{2}$ in Eqs. (C5)–(C7), the normalized Stokes parameters $\mathbf{S}_i'$ are obtained for $i = 1, 2, 3$, respectively, corresponding to the emerging states, expressed in the form

$$\begin{aligned}&\mathbf{S}_0' + \mathbf{e}_1\mathbf{S}_1' + \mathbf{e}_2\mathbf{S}_2' + \mathbf{e}_3\mathbf{S}_3' \\ &= 1 + \mathbf{e}_1\big(\cos 2\chi \cos 2\alpha' \\ &\quad + [\cos 2\chi \sin(2\alpha' - 2\theta)(1 - \cos\delta) \pm \sin 2\chi \sin\delta]\sin 2\theta\big) \\ &\quad + \mathbf{e}_2(\cos 2\chi \sin 2\alpha' - \big[\cos 2\chi \sin(2\alpha' - 2\theta)(1 - \cos\delta) \\ &\quad \pm \sin 2\chi \sin\delta]\cos 2\theta) + \mathbf{e}_3\left(\pm \sin\delta \cos 2\chi \sin(2\alpha' - 2\theta)\right. \\ &\quad \left. + \sin 2\chi \cos\delta\right).\end{aligned} \tag{C8}$$

The above equation corresponds to the emergent states generated by passing a polarized incident beam through a BE.

Acknowledgment. The authors are grateful for the financial support from the Vicerrectoría de Investigación y Extensión of the Universidad Industrial de Santander. The authors are grateful to Prof. P. Pellat-Finet for his valuable assistance.

Disclosures. The authors declare no conflicts of interest.

Data availability. The data underlying the experimental results presented in this article are available in [49]. There you will find the measured data of the emerging states, generated by the biplate in different configurations and for different incident states. The codes we use to obtain the graphics are also presented.

Supplemental document. See Supplement 1 for supporting content.

REFERENCES

1. C. Chou, Y.-C. Huang, and M. Chang, "Effect of elliptical birefringence on the measurement of the phase retardation of a quartz wave plate by an optical heterodyne polarimeter," J. Opt. Soc. Am. A **14**, 1367–1372 (1997).
2. G. Ghosh, "Dispersion-equation coefficients for the refractive index and birefringence of calcite and quartz crystals," Opt. Commun. **163**, 95–102 (1999).
3. R. N. Smartt and W. H. Steel, "Birefringence of quartz and calcite," J. Opt. Soc. Am. **49**, 710–712 (1959).
4. S. Pancharatnam, "Achromatic combinations of birefringent plates: part i. An achromatic circular polarizer," Proc. Indian Acad. Sci. A **41**, 130–136 (1955).
5. S. Pancharatnam, "Achromatic combinations of birefringent plates: Part ii. An achromatic quarter-wave plate," Proc. Indian Acad. Sci. A **41**, 137–144 (1955).
6. R. Bhandari and G. D. Love, "Polarization eigenmodes of a QHQ retarder—some new features," Opt. Commun. **110**, 479–484 (1994).
7. H. Gu, X. Chen, Y. Shi, H. Jiang, C. Zhang, P. Gong, and S. Liu, "Comprehensive characterization of a general composite waveplate by spectroscopic Mueller matrix polarimetry," Opt. Express **26**, 25408–25425 (2018).
8. D. Vala, P. Koleják, K. Postava, M. Kildemo, P. Provazníková, and J. Pivstora, "Effects of optical activity to Mueller matrix ellipsometry of composed waveplates," Opt. Express **29**, 10434–10450 (2021).
9. X. Zhang, "Optimal achromatic wave retarders using two birefringent wave plates: comment," Appl. Opt. **52**, 7078–7080 (2013).
10. H. Hurwitz and R. C. Jones, "A new calculus for the treatment of optical systems ii. Proof of three general equivalence theorems," J. Opt. Soc. Am. **31**, 493–499 (1941).
11. H. Poincaré, *Théorie Mathématique de la Lumière* (Gauthier-Villars, 1892), Vol. **2**, Chap. XII.
12. C.-J. Yu and C. Chou, "Characterization of a generalized elliptical phase retarder by using equivalent theorem of a linear phase retarder and a polarization rotator," Proc. SPIE **7934**, 79341F (2011).
13. C.-J. Yu, C.-E. Lin, Y.-C. Li, L.-D. Chou, J.-S. Wu, C.-C. Lee, and C. Chou, "Dual-frequency heterodyne ellipsometer for characterizing generalized elliptically birefringent media," Opt. Express **17**, 19213–19224 (2009).
14. P. Pellat-Finet, "Représentation des états et des opérateurs de polarisation de la lumière par des quaternions," Opt. Acta **31**, 415–434 (1984).
15. A. Saha, K. Bhattacharya, and A. K. Chakraborty, "Achromatic quarter-wave plate using crystalline quartz," Appl. Opt. **51**, 1976–1980 (2012).
16. J. L. Vilas and A. Lazarova-Lazarova, "A simple analytical method to obtain achromatic waveplate retarders," J. Opt. **19**, 045701 (2017).
17. A. Samoylov, V. Samoylov, A. Vidmachenko, and A. Perekhod, "Achromatic and super-achromatic zero-order waveplates," J. Quant. Spectrosc. Radiat. Transfer **88**, 319–325 (2004).
18. H. Gu, H. Jiang, X. Chen, C. Zhang, and S. Liu, "Superachromatic polarization modulator for stable and complete polarization measurement over an ultra-wide spectral range," Opt. Express **30**, 15113–15133 (2022).
19. L. Li and M. J. Escuti, "Super achromatic wide-angle quarter-wave plates using multi-twist retarders," Opt. Express **29**, 7464–7478 (2021).
20. M. Al-Mahmoud, V. Coda, A. Rangelov, and G. Montemezzani, "Broadband polarization rotator with tunable rotation angle composed of three wave plates," Phys. Rev. Appl. **13**, 014048 (2020).
21. A. A. Rangelov and E. Kyoseva, "Broadband composite polarization rotator," Opt. Commun. **338**, 574–577 (2015).
22. R. C. Jones, "A new calculus for the treatment of optical systems iii. The Sohncke theory of optical activity," J. Opt. Soc. Am. **31**, 500–503 (1941).
23. S. Saito, "$Su_{(2)}$ symmetry of coherent photons and application to Poincaré rotator," Front. Phys. **11**, 1225419 (2023).
24. C.-J. Yu, "Fully variable elliptical phase retarder composed of two linear phase retarders," Rev. Sci. Instrum. **87**, 035106 (2016).
25. S. Miller, L. Jiang, and S. Pau, "Generalized elliptical retarder design and construction using nematic and cholesteric phase liquid crystal polymers," Opt. Express **30**, 16734–16747 (2022).
26. X. Tu, L. Jiang, M. Ibn-Elhaj, and S. Pau, "Design, fabrication and testing of achromatic elliptical polarizer," Opt. Express **25**, 10355–10367 (2017).
27. J. J. Gil and R. Ossikovski, *Polarized Light and the Mueller Matrix Approach*, 2nd ed., Series in Optics and Optoelectronics (2022).
28. K. Salazar-Ariza and R. Torres, "Trajectories on the Poincaré sphere of polarization states of a beam passing through a rotating linear retarder," J. Opt. Soc. Am. A **35**, 65–72 (2018).
29. J. Pabón, K. Salazar, and R. Torres, "Characterization method of the effective phase retardation in linear birefringent thin sheets," Appl. Opt. **60**, 4251–4258 (2021).

30. R. M. A. Azzam, "Poincaré sphere representation of the fixed-polarizer rotating-retarder optical system," J. Opt. Soc. Am. A **17**, 2105–2107 (2000).
31. N. Wang and S. He, "A simple graphic method for analyzing the polarization state of an optical system with a fixed polarizer and a rotating elliptical retarder," Prog. Electromagn. Res. **174**, 107–114 (2022).
32. F. De Zela, "Two-component gadget for transforming any two nonorthogonal polarization states into one another," Phys. Lett. A **376**, 1664–1668 (2012).
33. S. G. Reddy, S. Prabhakar, P. Chithrabhanu, R. P. Singh, and R. Simon, "Polarization state transformation using two quarter wave plates: application to Mueller polarimetry," Appl. Opt. **55**, B14–B19 (2016).
34. D. Gottlieb and O. Arteaga, "Optimal elliptical retarder in rotating compensator imaging polarimetry," Opt. Lett. **46**, 3139–3142 (2021).
35. T. Tudor, "Vectorial Pauli algebraic approach in polarization optics. I. Device and state operators," Optik **121**, 1226–1235 (2010).
36. T. Tudor, "Vectorial Pauli algebraic approach in polarization optics. II. Interaction of light with the canonical polarization devices," Optik **121**, 2149–2158 (2010).
37. Q. Ke, K. Li, W. Wu, W. Li, H. Chen, R. Cai, and Z. Li, "Determination of birefringence of biological tissues using modified PS-OCT based on the quaternion approach," Front. Phys. **11**, 364 (2023).
38. C. Brosseau, *Fundamentals of Polarized Light: A Statistical Optics Approach* (Wiley, 1998).
39. R. C. Jones, "A new calculus for the treatment of optical systems i. Description and discussion of the calculus," J. Opt. Soc. Am. **31**, 488–493 (1941).
40. C. Whitney, "Pauli-algebraic operators in polarization optics*," J. Opt. Soc. Am. **61**, 1207–1213 (1971).
41. T. Tudor, "Interaction of light with the polarization devices: a vectorial Pauli algebraic approach," J. Phys. A **41**, 415303 (2008).
42. T. Tudor, "Vectorial pure operatorial Pauli algebraic approach in polarization optics: a theoretical survey and some applications," Appl. Opt. **51**, C184–C192 (2012).
43. M. Richartz and H.-Y. Hsü, "Analysis of elliptical polarization," J. Opt. Soc. Am. **39**, 136–157 (1949).
44. P. Pellat-Finet, "Geometrical approach to polarization optics: II. Quaternionic representation of polarized light," Optik **87**, 68–76 (1991).
45. P. Pellat-Finet, "Iterative experimental method for generating eigen-states and principal states of polarization," Appl. Opt. **51**, 4403–4408 (2012).
46. P. Pellat-Finet and M. Bausset, "What is common to both polarization optics and relativistic kinematics?" Optik (Stuttgart) **90**, 101–106 (1992).
47. K. S. Rao, K. S. Rao, and S. R. Koneru, *The Rotation and Lorentz Groups and Their Representations for Physicists* (Wiley, 1988).
48. J. del Hoyo, L. M. Sanchez-Brea, and A. Soria-Garcia, "Open source library for polarimetric calculations 'py_pol'," Proc. SPIE **11875**, 1187506 (2021).
49. J. Pabón, "Supplemental document for tunable birefringence and elliptical polarization eigenmodes in a biplate of two quarter-wave plates," figshare (2023), https://doi.org/10.6084/m9.figshare.24135483.v2.